Surface Structure and Reactivity: Reactions on Face-Centered Cubic (110) Metal Surfaces Involving Adatom-Induced Reconstructions

Maya Kiskinova

Sincrotrone-Trieste, Padriciano 99, 34012 Trieste, Italy

Received September 5, 1995 (Revised Manuscript Received January 9, 1996)

Contents

Dr. Maya Kiskinova began her research in surface chemistry and catalysis as a diploma student at the University of Sofia where she got her M.S. in 1972. As a graduate student she continued her studies on chemisorption on metals. She got her Ph.D. in Physical Chemistry in 1977 and her Sc.D. degree in 1989 in the Bulgarian Academy of Sciences, where she worked until 1990. During the period 1980–1990 she worked for long periods as a visiting scientist at the National Bureau of Standards and at the University of Pittsburgh in the United States and at the Scientific Center of Juelich in Germany. Presently, she is a group leader at the ELETTRA Laboratory in Sincrotrone-Trieste (Italy), a position which she has held from 1991. Her research activity covers studies on single-crystal metals and semiconductors, thin films, and oxide and silicide interfaces using wide range of surface sensitive spectroscopies and local probe techniques. Her research is focused on understanding processes involved in the structural and chemical transformations of chemisorbed systems on model metal catalysts and their relation to surface reactivity and in the chemical modifications of semiconductor surfaces.

1. Introduction

Over the past 30 years the rapid development of surface science techniques has led to remarkable progress in the understanding of the phenomenon catalysis, which is a complex system of various processes. Catalysis can generally be divided into four interrelated processes: adsorption, desorption, surface and subsurface diffusion, and interaction between coadsorbed atoms, molecules, and molecular fragments. It has been recognized that any foreign adsorbed species changes the local surface properties. In milder cases the adspecies modify the electronic structure of the substrate surface atoms with negligible changes in their equilibrium positions. In more severe cases creation of more suitable surface sites is required, which results in a completely changed substrate surface structure. That is why structural variations of the working catalyst surface, induced by the reaction participants, occur quite frequently and can result in nonlinear dynamics and kinetic oscillations.[1−3]

A real catalyst surface consists of "microsurfaces" of various crystallographic orientations. Going from low- to high-index faces the number of the nearest-neighbor broken bonds increases, resulting in a higher surface free energy. This makes the higher index planes less resistive toward restructuring in the presence of strongly bound adsorbates. It appears that for a great number of surface reactions the higher index planes exert a higher activity and can be classified as preferred faces for the catalytic reactions. Hence, the possible structural variations

S0009-2665(95)00226-3 CCC: $25.00

of these preferred faces, induced by chemisorbed reaction participants, are expected to play an important role in the reaction pathway. This has motivated the increasing scientific interest in reconstructive chemisorption, which is a starting point to reveal the relation between surface structure and chemical reactivity. Despite the short history of quantitative studies of adsorbate-induced surface reconstructions, serious reviews on this subject already exist.[4−9]

Probing the structural and compositional changes occurring on the catalyst surface at a microscopic scale and under dynamical conditions is one of the most recent exciting challenges of surface science studies. It has been stimulated by the development of advanced techniques, such as scanning tunnelling microscopy (STM) and photoemission electron microscopy (PEM). These techniques can explore the surface processes in real time and at a microscopic scale, ranging from a few micrometers to atomic resolution. STM provides information on the surface structure and dynamic processes on the surface at atomic level and in real space.[10] When probing a metal surface in the conventional constant low-current mode the STM images can often be simply interpreted as topographic maps. Depending on the induced changes in the local density of states at the Fermi level the adsorbates may appear as protrusions or depressions in the STM images. PEM probes a laterally varying adsorbate concentration based on the dependence of the photoelectron yield on the local work function determined by the adsorbates.[11] The spatial resolution of a few micrometers allows the effect of the local surface structure and composition on the propagation reaction fronts (named chemical waves) to be studied. The STM and PEM studies have proved that the reaction mechanism is governed by the variations of the catalyst surface structure and composition occurring at a microscopic level. In the traditional description, these variations should determine the type and density of the so-called "active" surface sites. Last decade considerable progress in this respect was made in model studies of adsorption and surface reactions on single-crystal surfaces of face-centered cubic (fcc) metals (Cu, Ag, Ni, Pd, Rh, Pt, etc.), which represent a very important class of catalysts. A common feature of the obtained results is the structural and compositional nonuniformity of the working metal surface, predicted by Taylor ~70 years ago[12]. Figure 1.1 illustrates an example of structural and compositional heterogeneity, evidenced by STM during neutralization of NO on a Rh-(110) surface. As can be seen the local surface reactivity should be controlled by the adsorbed O and N, which segregate in islands with a different local structure.

Here, the most recent achievements, which have shed light on the microscopic mechanism of surface reactions are reviewed. Emphasis is placed on the contribution of local probe techniques in providing insight into the mechanism and dynamics of surface reactions. Two interrelated topics are addressed, namely adatom-induced reconstructions and reactions involving adatom-induced reconstructions. Representative examples of adsorption and reaction studies performed on the fcc (110) metal planes are selected to illustrate the correlation between surface structure and reactivity.

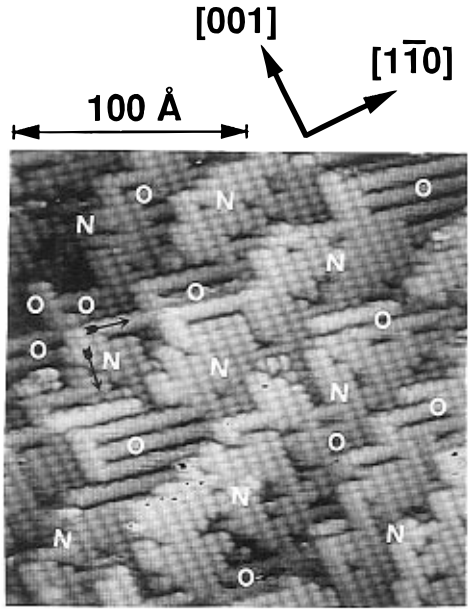

Figure 1.1. STM image observed during dissociation of NO on a Rh(110). The N-phase consists of rows running in the [001] direction. The O-phase consists of rows running in the [1$\bar{1}$0] direction.

The article has been organized in a systematic manner. In sections 2 and 3 reconstructive interactions of adatoms with metal substrates are summarized. These interactions are important reaction steps in the catalytic reactions reviewed in section 4. The adatom-induced surface restructuring in several single- (section 2) and double- (section 3) component adsorbate systems is briefly described. The focus is on the factors controlling the reconstruction processes and the microscopic mechanism of formation of the new surface phase. The similarities and the differences between adsorption systems will be discussed, emphasizing on the role of adsorbate and substrate nature and the influence of other coadsorbed species. Section 4 addresses the recent research effort and success in identifying the main operating microscopic mechanisms in surface reactions, involving reconstructive chemisorption. Several oxidation reactions are selected to illustrate the common characteristics and the complex set of events which occur on the catalyst surface. Particular attention is given to the recent findings about the nature of the preferred reaction sites on a reconstructed surface and about the local structural and compositional variations in the course of the reaction. Several representative examples illustrate the impact of the surface structure on the reactivity. Finally, a brief summary and some remarks about directions for future research are given in section 5.

2. Reconstructions of fcc (110) Surfaces: Single-Adsorbate Systems

2.1. General Remarks

Adatom-induced reconstruction of higher index faces of the transition metals appears to be a general

phenomenon with the type of surface reconstructions varying with different adsorbates and substrates. The adsorbate and substrate nature and the substrate surface symmetry are operating factors in the reconstruction phenomenon where processes, such as bond breaking, bond formation, and surface diffusion, are involved. In many cases thermal activation and a critical adatom coverage are needed to overcome the activation barriers of these elementary steps. Presence of coadsorbates can also affect the reconstruction process by changing the activation barriers for bond breaking, bond formations and surface diffusion.

Thermodynamically the driving mechanism of reconstruction is a lowering of the surface free energy, which is determined by enthalpy and entropy variations.[13] Assuming that the enthalpy term is dominating, the reconstruction should be favored if the energy cost for reconstruction is compensated by the energy gain from the stronger adsorption bond on the reconstructed surface. Although the entropy term associated with adsorbed species is usually small its contribution should also be considered, especially in cases when the chemisorption energy gain is not very large. Larger entropy variations can be provoked by changes in the interlayer spacing, created edges at the exposed microfacet, modified adsorption sites, etc. The kinetic of reconstruction is controlled by coverage and temperature-dependent factors, including activation energies of bond breaking and/or bond formation, activation energies of surface and/or bulk diffusion of the adsorbed species, substrate atoms, etc. That is why even a thermodynamically favored reconstruction process can be kinetically hindered at low temperatures and adsorbate coverages or in the presence of other coadsorbed species.

The microscopic mechanism of reconstruction can differ substantially with different systems. In some cases the new reconstructed phase grows homogeneously on flat terraces, whereas in others it grows preferentially at step edges. In some systems the nucleation of the new phase starts with the first adsorbed species, in others accumulation of a critical adsorbate coverage is needed before the surface is distorted. Also the local mechanism of displacement and mass transport of the surface atoms varies substantially with different systems. This information for the elementary steps is of importance when the energy cost of reconstruction is valued. For example, recent STM results have revealed a mechanism where the new structural units of a reconstructed phase are formed by metal atoms supplied at a lower energy cost from the lower coordinated "defect" sites, e.g. step edges, kinks, etc.[4,6]

Of the three most studied faces of the fcc metals, (111), (100), and (110), the (110) face is the least stable and it quite often undergoes reconstructions. This has motivated the present selection of reconstructive interactions on fcc (110) surfaces to illustrate the impact of the surface structure on the chemical reactivity. Common adsorbate-induced reconstructions of the fcc (110) planes are the "so-called" $(n\times1)$ and $(1\times n)$ "missing-row" reconstructions, where [100] or [$1\bar{1}0$] rows are absent, respectively. "n" is an integer with values ≥ 2. The periodical absence of [100] or [$1\bar{1}0$] rows results in exposing of the (100) or (111) facets, respectively. Since the closed-packed (111) facets have a lower surface free energy than the (100) facets, the $(1\times n)$ reconstructions should be energetically more favorable.[13] However, this general consideration justifies only the $(1\times n)$ reconstructions of the clean (110) planes. In adsorption systems the adatom bonding configuration plays an important role, and as will be shown below, it often favors the $(n\times1)$ reconstructions.

2.2. Adatom-Induced ($n\times1$) and ($1\times n$) Reconstructions

The systems described in this subsection are selected because of their relevance to the surface reactions discussed later on. The adsorbates are the highly reactive elements, O, N, and S, which participate as adatoms in many important metal-catalyzed reactions, ranging from purification of exhaust gases to important industrial synthesis of ammonia, nitric acid, oxygenates, etc. The substrates under consideration are several transition metals, namely Rh, Pd, Ag, Cu, and Ni, used as catalysts in these syntheses. The adsorbate bond energies of O, N, and S on these transition metals are comparable to the bond energies between the substrate atoms.[14] This favors reconstructive chemisorption provided the stronger bonding obtained with the new surface structure compensates for the energy loss from breaking the metal−metal bonds.

2.2.1. Oxygen-Induced Reconstructions

The most thoroughly studied class of adsorbate-induced reconstructions is that of oxygen chemisorption on the fcc (110) transition metal surfaces, reviewed thoroughly recently in refs 4 and 15. STM has successfully been used to prove the O-induced surface reconstructions on Cu(110),[16−18] Ni(110),[19] Ag(110),[20] Rh(110),[21] and Pd(110).[22]

The fcc (110) surfaces of Cu, Ni, and Ag undergo $(n\times1)$ reconstructions even upon room temperature oxygen adsorption. The structural units of the reconstructed surface are [001] metal−oxygen (−M−O−) chains with oxygen located in a long bridge position between two metal atoms.[15] Some of the adlayer structures, involving $(n\times1)$ reconstructions, are schematically shown in Figure 2.1.

The interaction of O with Rh(110) and Pd(110) surfaces results in the other type of reconstruction, $(1\times n)$. The structural units are [$1\bar{1}0$] −M−O− chains with O located in the 3-fold sites along the rows in a zigzag arrangement. Figure 2.2 presents schematic models of some of the O-$(1\times n)$ phases observed on Rh(110).

For both types of reconstruction the density of the −M−O− chains and the lattice spacing between them change with increasing oxygen coverage. In some systems, where the −M−O− units are mobile, the weak attractive interactions between them result in formation of phase-segregated domains of ordered $(n\times1)$ or $(1\times n)$ structures at rather low coverages.

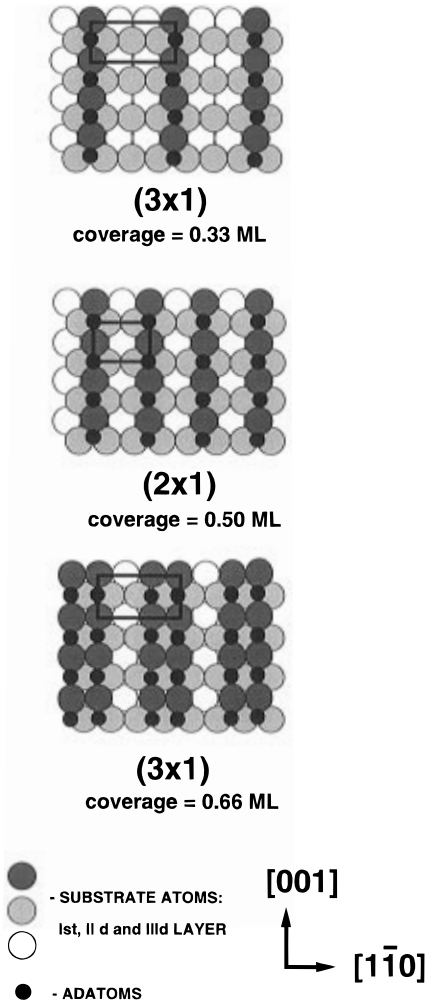

Figure 2.1. Structural models of the most common ($n\times1$) reconstructions induced by O or N on fcc(110) Ni, Ag, Cu, and Rh: top, primitive (3×1); middle, primitive (2×1); and bottom, nonprimitive (3×1).

2.2.2. Nitrogen- and Sulfur-Induced Reconstructions

The reconstructive interactions of nitrogen with the fcc(110) transition metal surfaces are less thoroughly studied.[4] The STM results have evidenced that, similar to oxygen, nitrogen also induces reconstructions involving absence of [001] or [1$\bar{1}$0] rows.[23−26] For Cu(110) and Ni(110) the N-induced structure involves absence of every third [1$\bar{1}$0] row with a double periodicity in the [1$\bar{1}$0] direction due to N adsorbed in a long bridge site.[23−25] On Rh(110) the N-induced ($n\times1$) structures are similar to those observed for O on the (110) faces of Cu, Ni, and Ag for coverages ≤ 0.5 monolayer [26] (see Figure 2.1). One monolayer (ML) equals the number of substrate atoms on an unreconstructed surface.

The sulfur-induced reconstructions were studied by STM only on a Ni(110) surface, where the chemisorbed S layers were produced by decomposition of H_2S.[27] As opposed to oxygen, deposition of S at room temperature results in a S-c(2×2) layer at 0.5 ML on an unreconstructed Ni(110) surface. Structural changes were evolved only at elevated temperatures resulting in a S-(4×1) reconstructed phase at ∼0.75 ML. Similar to the case of O on Ni(110), [001] rows are the structural units of the S-(4×1) phase: two [001] rows for every four ⟨110⟩ (1×1) lattice spacings.

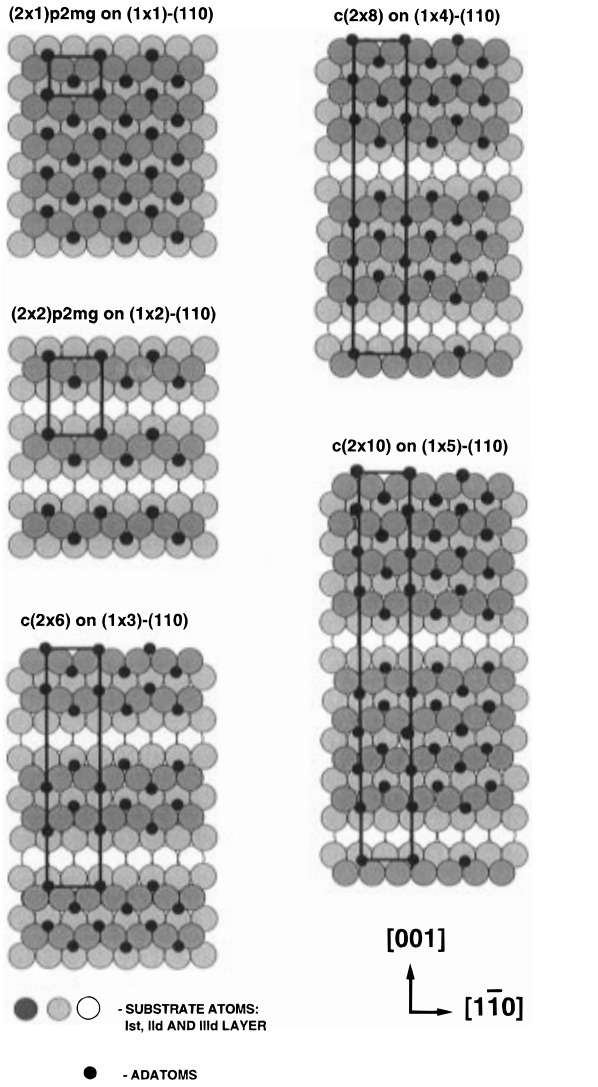

Figure 2.2. Structural models of O chemisorption on an unreconstructed (1×1)-Rh(110) and reconstructed ($1\times n$)-Rh(110) surfaces.

2.3. Elementary Steps Involved in the Reconstruction Process

2.3.1. (n×1) Reconstructions

The processes involved in the formation of a new reconstructed phase, namely surface diffusion of adatoms, nucleation, and growth, depend on many factors. For the same adsorbate−substrate system the time scale for these events depends on the adsorbate and substrate−adatoms supply rates and surface diffusion rate, which are strongly temperature dependent. In the particular cases of surface reconstructions under consideration, where the adsorbate is supplied from the gas phase, the adsorbate supply rate depends on the gas flux and sticking probability. Much insight in the microscopic mechanism of reconstruction has been gained from STM "snapshots" during the nucleation and growth process. However, it should be noted that the collected data describe the processes occurring in a rather narrow temperature range (300−450 K), when the formation of the reconstructed phase can be considered irreversible due to the negligible desorption rate of the adsorbate.

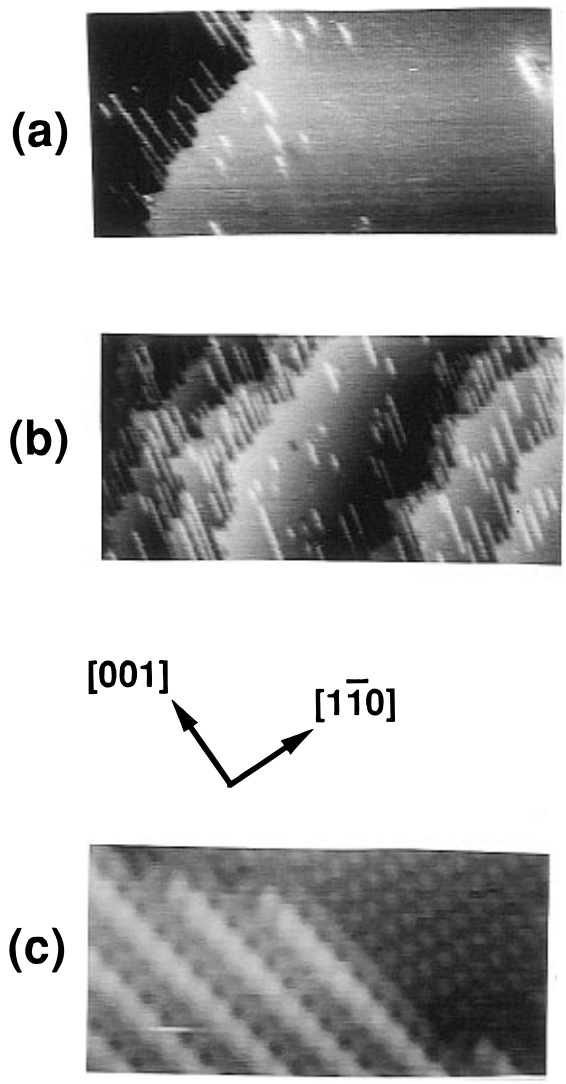

Figure 2.3. STM images of Rh(110) with adsorbed N, deposited by NH_3 exposure at 430 K. Panels a and b represent regions with a different step density which reflect the predominant growth of the added [001] −Rh−N− chains (bright lines) at the step edges. Panel c illustrates a high-resolution STM image of coexisting (1×1) bare surface and N-(3×1) "added-row" domains. The position of the bright round features is consistent with imaging of Rh atoms.

Recent STM dynamical studies have revealed that the [001] −M−O− and −M−N− structural units of the (n×1) phase nucleate and grow following the so-called "added-row" mode.[15,16,26] This has been evidenced directly by STM, as shown in Figure 2.3. The STM images in Figure 2.3 are taken during development of the N-(n×1) phase on Rh(110). The added [001] −Rh−N− rows are imaged as bright strings.[26] The only difference observed during the growth of the O-(n×1) phases on Cu, Ni, and Ag is the higher density of added rows on the terraces. According to the "added-row" mechanism the substrate adatoms, supplied from the step edges and terraces, are trapped by the adsorbed foreign atoms (O, N, or S) to form the [001] units.[16] Usually, terraces contribute less to the adatom supply, because the removal of a highly coordinated substrate atom from the terraces requires a higher energy. A common feature of the O- and N-(n×1) reconstructions under consideration is that they do not require a critical adsorbate coverage. This indicates that provided the influence of other coadsorbed species is negligible, the surface reactions involving chemisorbed O or N proceed always on reconstructed surfaces.

The added-row (n×1) reconstructions can be described as a three-step process: (1) supply of adsorbate from the gas phase and of substrate adatoms from the step edges or terraces; (2) interaction of the substrate adatoms with the adsorbate resulting in nucleation and growth of [001] −M−X− units, where M is metal and X is O or N; (3) agglomeration of the −M−X− units in (n×1) islands. At the same reaction temperature the relative amount of substrate adatoms, supplied by the step edges and terraces, and the mobility of these adatoms and of the formed −M−X− chains vary with the adsorbate−substrate system and the adsorbate coverage. If the supply of an adsorbate from the gas phase and trapping of the substrate adatoms by the adsorbate are fast enough, the rate-limiting processes remain the creation of substrate adatoms and the diffusion of the released substrate adatoms and of the −M−X− structural units. If the supply of substrate adatoms is facile and the mobility of the created adatoms is high, the new added-row phase nucleates and grows homogeneously on the terraces. This mechanism is followed by the (n×1)-O reconstructions on Cu, Ag, and Ni at room temperature. In contrast, if the substrate adatom supply and diffusion rates are low, heterogeneous nucleation and growth dominate. A typical example for heterogeneous growth is the (n×1) N-induced reconstruction on Rh(110), where most of the −Rh−N− units remain attached to the terrace boundaries (see Figure 2.3). As will be discussed below, the homogeneous growth of [001] −Rh−N− chains on the terraces is limited by the low rate of Rh adatom displacement and transport from the step edges. At higher coverages, when the −Rh−N− chains saturate the step edges, the negligible supply of Rh adatoms from the terraces prevents the complete transformation to a (2×1)-N phase.[26] It should be noted that these results describe the microscopic mechanism of N-(n×1) reconstructions in the temperature range 300−450 K. Provided the adsorbate supply remains high enough, the growth mechanism can become homogeneous at higher temperatures, because both the supply rate and the diffusion rate of the substrate adatoms will increase. This means that more substrate adatoms will be created, which can diffuse longer distances to form added rows onto the terraces.

The attractive M−X interaction within the −M−X− rows accounts for the faster growth rate of the reconstructed phase in the [001] direction. Formation of islands with a preferred (n×1) periodicity depends on the mobility of the −M−X− units and on the relative strength of the repulsive and attractive forces between them. A tendency to early formation of (n×1) islands is typical for the O reconstructive chemisorption on Cu, Ag, and Ni at room temperature, where the substrate adatoms and the −M−O− units are rather mobile. The increase in the mobility of the longer −M−O− chains and islands at higher temperature results in aggregation and better ordering.[18] In contrast, N reconstructive chemisorption on

Rh(110) at temperatures < 450 K shows random growth with no tendency to island formation of a particular N-($n\times1$) phase at low coverages. This behavior is related to the low mobility of the Rh adatoms and the −Rh−N− units at <450 K.

In the temperature range and for the adsorbate fluxes considered here the above outlined differences in the ($n\times1$) "added-row" growth mode on different substrates can be explained by suggesting that the first reaction step, namely the supply of substrate adatom, plays a dominant role. The activation energies of creation and surface diffusion of the substrate adatoms are specific for each substrate because they are determined by the metal−metal bond strength. The latter is 144, 177, 203, and 286 kJ mol^{-1} for Ag, Cu, Ni, and Rh, respectively.[28] Obviously, the relatively large energy cost for breaking the Rh−Rh bonds accounts for the dominating supply of Rh adatoms from the step edges where the coordination is lower. The fact that a great number of the formed −Rh−N− added rows remains attached to the terrace boundaries indicates that even the displacement and diffusion of Rh atoms from the step edges are impeded. This results in the observed heterogeneous growth of the new ($n\times1$) phase on Rh(110), in contrast to the homogeneous growth observed on the other three metals. The relatively high activation barrier for diffusion also limits the mobility of the −Rh−N− units. Hence, islands of the preferred (3×1) and (2×1) phases are formed only at higher N coverages, when the increased −Rh−N− chain density leads to compression. The above considerations reveal to a great extent why within a certain temperature range, at which the supply and the lifetime of the adsorbate are still high, the reconstructions become more facile at higher temperatures. This trend correlates with the activation barriers for breaking metal−metal bond, for atom rearrangement processes, and for surface diffusion of the adparticles. As outlined above and will be discussed later on, changing the reaction conditions, e.g. temperature, adsorbate supply, or presence of other adspecies, can also convert over to other reconstruction mechanisms or hinder the reconstruction process.[4,7,26]

2.3.2. (1×n) Reconstructions

A combined missing/added-row mechanism governs the ($1\times n$) reconstructive interactions: the substrate atoms removed from step edges or terraces create missing rows along the [110] direction, as illustrated by the STM image in Figure 2.4a. In principle the ($1\times n$) reconstructions can be described by the same three-step mechanism acting in the ($n\times1$) added-row reconstructions. The only difference is that there is a directional preference in the substrate adatoms removal leading to the formation of [1$\bar{1}$0] troughs (missing rows). This directional removal of substrate atoms is energetically justified because it involves breaking of less nearest-neighbor metal−metal bonds. A rather distinguishable feature of the ($1\times n$) reconstructions is the very extended length of the [1$\bar{1}$0] missing and added rows resulting in a highly anisotropic growth of the ($1\times n$)-phase islands. In contrast to the ($n\times1$) reconstructions, the preferred adsorption site in the ($1\times n$) phase varies with the adsorbate: on

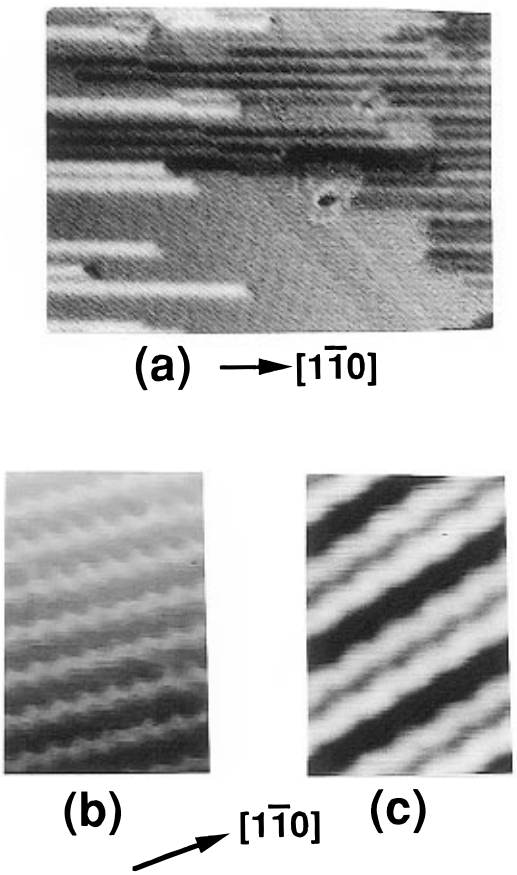

Figure 2.4. (a) STM image taken during the growth of a O-(1×2) reconstructed phase on Rh(110). (b) STM image of the O-(2×2)p2mg phase on Rh(110). (c) STM image of the O-c(2×6) phase on Rh(110). The zigzag shape of the −Rh−O− chains, imaged as bright features in b and c, reflects the arrangement of O along the [1$\bar{1}$0] rows.

Rh(110) and Pd(110) the oxygen occupies fcc 3-fold sites along the [110] rows[21,22] (see Figure 2.2), whereas in the (2×3) structure on the (1×3) reconstructed Cu(110) the nitrogen occupies each second long bridge site between two [1$\bar{1}$0] rows.[23,24] This means that in the case of ($1\times n$) reconstructions the adsorbate bonding configuration cannot be considered as a dominant factor for preferential directional growth of the reconstructed phases. Most likely the higher diffusion rate of the adatoms along the smoother [1$\bar{1}$0] direction accounts for the formation of long [1$\bar{1}$0] chains also in the case of the long-bridge-bonded N on (1×3)-Cu(110).

2.4. Reconstruction and Bonding Configuration

The ($n\times1$) and ($1\times n$) reconstructions, described above, result in a lower metal−metal coordination number and a stronger bonding of the adsorbate. The stronger bonding, acting as a driving force for reconstruction, suggests enhanced hybridization between the metal valence electrons (usually levels in the surface d band for transition metals) and the adatom valence levels (2p for N, O, and S). Indeed, the effective medium theory calculations, performed recently, have shown that when the metal−metal coordination number decreases, as is the case of ($n\times1$) and ($1\times n$) reconstructed surfaces, the metal d band moves closer to the Fermi level resulting in enhanced hybridization between the metal d states

and the valence states of the adsorbate.[27,29] According to these theoretical calculations the favored bonding configuration is the one that ensures an optimum electron density. In the particular case of strongly bonded adsorbates with small atomic sizes, such as O and N, the new created adsorption sites should have a larger surrounding electron density. This can be attained by moving the adatoms closer to the metal atoms. Indeed, the bridge-bonded N and O in the [001] added −M−X− rows show a tendency to move deeper in the outermost metal layer, which results in expansion of the metal first interlayer spacing.[4,15,24] In the case of $(1\times n)$ reconstructions the absence of a $[1\bar{1}0]$ row causes slight displacement of the substrate atoms (buckling and row-pairing) so that the oxygen adsorbed along the (1×2) troughs can be more deeply embedded in the preferred 3-fold sites at the rudimentary (111) face.[30] This results in an enhanced bond energy on the (1×2) reconstructed surface, which is consistent with the slightly higher normal and parallel vibrational frequencies measured for O in the 3-fold sites on a reconstructed Rh(110) surface.[31] The embedding becomes more facile going to substrates with a larger lattice constant. When the adatoms have relatively small atomic radii the "reconstructive" chemisorption can be accompanied by penetration below the outermost substrate layers. This is quite common for O and N, which adds to the structural effect on the chemical reactivity. In the most severe cases the surface reconstruction can involve local formation of surface compounds (oxide, nitride, sulfide).[4,15] These complex variations of the adsorbate bonding configuration controls the reaction energetic, where the values of the bond energies are a dominant factor.

An interesting feature of the systems under consideration is that for the same substrate the N-driven reconstructions are orthogonal to that induced by oxygen. This can be interpreted considering the reconstruction process as an intermediate state to compound formation. Hence, the type of reconstructions should mimic the corresponding compound-like structures, which are often different for nitrides and oxides.

2.5. Factors Controlling the Growth Mode of the Reconstructed Phases

To analyze the factors that influence the growth of a reconstructed phase one should consider mainly those who can affect the energetic involved in the reconstructive interactions. In a simplified picture these are the energy gain from reconstruction, ΔE_r, which can be presented as a difference between the gain in M−X chemisorption energy on a reconstructed surface, ΔE(M−X), and the energy loss for breaking metal−metal bonds, E(M−M):

$$\Delta E_r = \Delta E(\mathrm{M-X}) - E(\mathrm{M-M})$$

According to this equation the energetic should be determined by the M−M and M−X bond strengths. The second term, E(M−M), depends also on the type and the number of broken M−M bonds. The quantities of ΔE(M−X) and E(M−M) can be influenced by the adsorbate coverage, by the penetration of the adsorbate subsurface and by the local environment, e.g. the presence of other coadsorbed species.

Considering the energetic involved in the reconstructive interactions, one can explain why the growth mode of the $(n\times 1)$ and $(1\times n)$ phases differs. The dominating added-row mechanism in the $(n\times 1)$ reconstructions correlates with the higher energy barrier for creation of a [001] trough because this process involves net breaking of nearest-neighbor metal−metal bonds. This explanation is consistent with the recent STM studies of O chemisorption on Ni(110), where a second reaction channel involving growth of long strings and creation of troughs along the $[1\bar{1}0]$ direction is evidenced at a low-oxygen coverage.[15,19] This second channel resembles the added/missing row mode of the O-induced reconstruction on Rh(110). The $[1\bar{1}0]$ −Ni−O− chains spontaneously dissolve and transform into added [001] −Ni−O− rows above a certain critical oxygen coverage. The fact that this reaction channel cannot be observed at elevated temperatures indicates that the $[1\bar{1}0]$ −Ni−O− chains should be considered as a metastable intermediate state. It is likely that the weaker O bonding in this metastable reconstructed phase on Ni(110) is compensated by the lower energy cost for the $(1\times n)$ reconstruction. The increase of oxygen coverage obviously changes the energy balance in favor of the more stable −Ni−O− [001] rows. Again energetic considerations can account for the absence of a similar second reaction channel during the O-$(n\times 1)$ reconstructive interactions on Cu and Ag: for Ni the oxygen chemisorption energy gain on a $(n\times 1)$ reconstructed surface, ΔE(M−O), is smaller, whereas the energy loss for breaking metal-metal bonds, E(M−M), is larger.[15]

Small ΔE(M−O) and relatively high E(M−M) values can also explain the requirement for a critical adsorbate coverage to initiate a reconstruction process, observed in the case of O-$(1\times n)$ reconstructions on Rh(110) and a S-(4×1) reconstruction on Ni(110). For oxygen on Rh(110) the HREELS and fast-XPS data have shown that the in the temperature range 120−570 K the occupation of the fcc 3-fold sites is always preceded by adsorption in other sites at low coverages.[31] This means that at low coverages, when the O−O repulsions are negligible, the difference between the Rh−O bond strength on a reconstructed and unreconstructed surface, ΔE(Rh−O), is not large enough to favor an immediate reconstruction. Certain accumulation of oxygen is necessary to change the energy balance in favor of a reconstructed surface with oxygen located at the fcc 3-fold site. Another important result from the HREELS and fast-XPS studies is that the initial reconstruction steps might involve oxygen incorporation below the outermost layer. This distorts the substrate lattice and, by reducing the E(M−M) value, facilitates the displacement of the Rh atoms at a lower energy cost.

The last factor that can influence considerably the rate and the mechanism of adatoms-induced reconstructions is the presence of coadsorbates. The coadsorbate effect is scarcely studied, although it is of great importance for understanding of mechanism of surface reactions, where several species compete

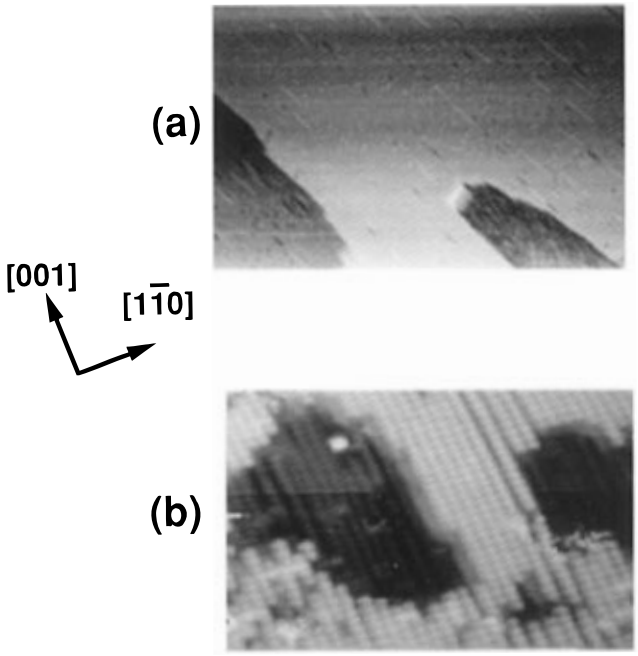

Figure 2.5. (a) STM image taken during nucleation of −Rh−N− units on Rh(110) in the presence of oxygen: bright and dark lines are added and missing [001] rows, respectively. (b) A N-(2×1) phase produced after removal of O from a saturated O + N coadsorbed layer: formation of islands located at two levels is evidenced.

for the surface sites. The coadsorbate can "activate" or "deactivate" the surface reconstruction. "Activation" effect of coadsorbed O on the N-induced reconstruction on Rh(110)[26,32] and on the S-induced reconstruction on Ni(110)[33] has been reported. In the case of N/Rh(110) the promotion effect of oxygen is ascribed to destabilization of the substrate surface by the chemisorbed or subsurface oxygen. This results in lowering the activation barrier for removal and diffusion of the Rh atoms. The coadsorbates can also change the reconstruction mode. As shown in Figure 2.5, in the presence of O the added [001] −Rh−N− rows grow on the terraces: the removed Rh atoms form the top layer of added [001] rows leaving [001] troughs behind. This growth mechanism differs from the "added-row" mode observed in the absence of O, where the step edges are the major supply of Rh adatoms (see Figure 2.3).[26] Consequently the coadsorbed oxygen switches on a homogeneous growth mode of the [001] −Rh−N− units onto the terraces by a combined missing/added row mechanism. The mechanism of the O-activated S-induced reconstruction on Ni(110) is different. The presence of oxygen constrains adsorption of S on large flat areas resulting in a rougher surface which reconstructs at a lower energy cost.[33]

3. Reconstructions in Coadsorbed Systems

3.1. General Remarks

In order to predict how the surface will respond to the complex chemical environment under various reaction conditions the role of site competition, of lateral interactions between each species and of local surface properties has to be known. Complicated reaction systems, where reconstructions are favored by several adsorbates, exist even in simpler cases, e.g. dissociation of heteronuclear molecules, such as NO, CO, etc. That is why one cannot draw a dividing line between coadsorbed systems and surface reactions, i.e. the coadsorbed systems can be considered as the simplest case of a surface reaction.

When each of the coadsorbates induces a reconstruction, the interactions between differing and similar units building the reconstructed surface phases should be considered. The atomic adsorbates under consideration can be classified as electronegative species. This predicts competitive adsorption if the repulsive interactions between the differing units are stronger than those between the similar units. The phase separation in these cases means that there is a net repulsive interaction between the structural units of differing reconstructed phases. As outlined above, strong attractive "Me−X" interactions along the chains and weak attractive interactions between the chains exist in the ($n\times1$) and ($1\times n$) single-adsorbate systems. These interactions favor a phase separation in coadsorbate systems.

Typical examples of competitive adsorption are the systems: O + N on Cu(110),[34] O + H on Ni(110),[35] and O + N on Rh(110),[36,37] where the coadsorbates induce orthogonal reconstructions. Directional growth of M−O and M−N(H) islands, rotated 90° with respect to each other, is the common feature of these systems (see, e.g., Figure 3.1b).

3.2. Formation of Separate Reconstructed Phases

In these coadsorption systems the surface is divided between the coadsorbate phases resulting in structural and compositional heterogeneity of the surface. The size of the domains usually does not exceed few tens of angstroms, which implies variations of the surface properties at a nanometer scale. Typical examples are the systems N + O/Cu(110) and O + H/Ni(110), where each adsorbate forms separate domains of a reconstructed surface.[34,35] The two reconstructed phases interact weakly and coexist until saturation. In the case of N + O on Cu(110), when the surface partly covered by islands of a N-(2×3) phase is exposed to oxygen, the chemisorbed oxygen forms its own domains of a (2×1) phase without affecting the existing N-(2×3) islands.[34] In the system O+H on Ni(110) the difference is that the growing [1$\bar{1}$0] −Ni−H− chains affect the O-($n\times1$) domains: they induce local compression of oxygen into a (2 × 1) phase and reduce the coherence of the larger oxygen islands by crossing through them.[35] It should be noted that the coexistence of O and H reconstructive phases on Ni(110) is possible only at room and low temperatures. At the higher reaction temperatures of H_2O formation the H reconstruction is lifted and the surface reactivity is affected only by the properties of the oxygen-($n\times1$) reconstructed phase.

3.3. Competitive Reconstructive Interactions

A typical example for competitive reconstructive interactions is the N + O coadsorption on a Rh(110) surface. The coadsorbed N + O layer on Rh(110) carries the common feature of formation of two

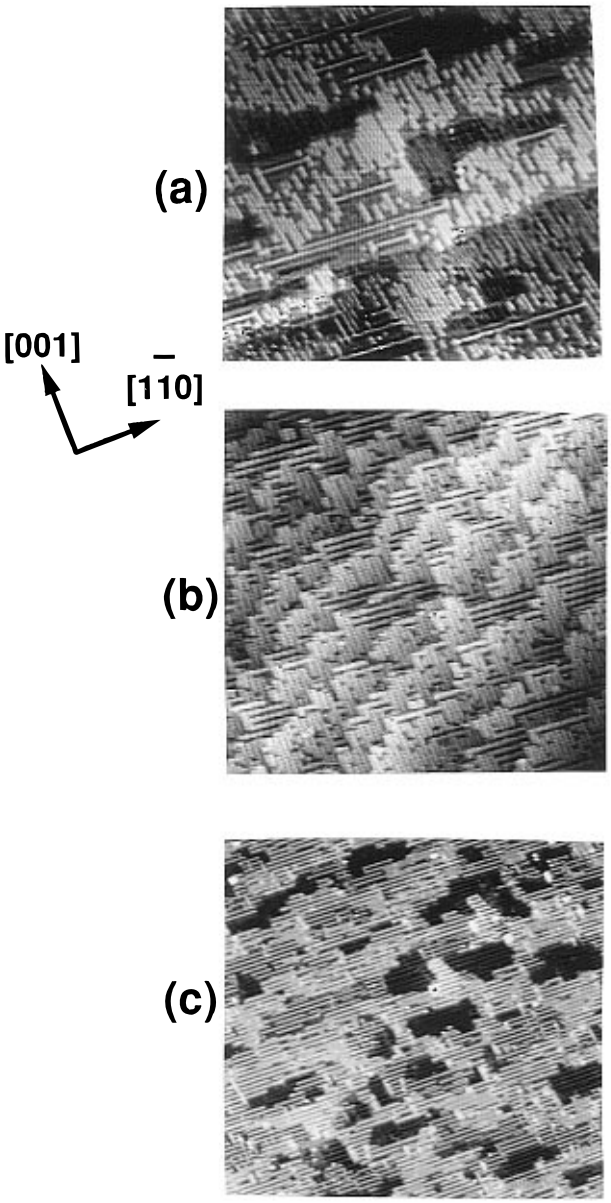

Figure 3.1. (a) STM image of a N + O layer (~0.2 ML) on Rh(110) where the N-(3×1) phase dominates: the basic units, [001] -Rh-N- chains, and a few long [1$\bar{1}$0] −Rh−O− chains, are imaged as bright lines. (b) STM image of a N + O layer (~0.5 ML) on Rh(110) showing a surface shared between N-(2×1) and O-(1×2) islands. (c) STM image of a N + O layer (~1 ML) on Rh(110) showing a (1×2) reconstructed surface.

reconstructed phases only in a narrow coverage range, because there is a competition between the coadsorbed atoms for dominating the surface structure.[36,37] The interactions observed during coadsorption of O and N on Rh(110) can be classified as a surface reaction leading to destabilization and easier removal of the reaction product N_2. This system is interrelated with the NO neutralization reaction in the exhaust gas converters, where the adsorbed O and N are the most strongly bonded intermediates. The surface science studies have revealed that depending on the actual reaction conditions, i.e. the reactants partial pressures and temperature, the phases dominating the surface properties can be N-(n×1), O-(1×n), or mixed N-(n×1) + O(1×n), respectively.[26,32,36−38]

The same phase transformations have been observed in experiments of O coadsorption onto a N-(n×1) layer at ~400 K[26] and of simultaneous coadsorption by NO dissociative adsorption.[32,36,37] The STM images in Figure 3.1, taken after different NO exposures, reveal the competition between the N-(n×1) and O-(1×2) reconstructive interactions with increasing the coadsobate coverage. The conversion occurs from a dominating (3×1)-N phase at low O + N coverages (Figure 3.1a) via an intermediate state of separate (2×1)-N and (1×2)-O islands (Figure 3.1b) to a c(2×4) phase formed by a c(2×2) O + N adlayer on a (1×2) reconstructed surface (Figure 3.1c). As discussed in subsection 2.5. and shown in Figure 2.5, at the beginning of the reaction the N-(n×1) phase grows homogeneously according to a missing/added-row mechanism, favored by the presence of coadsorbed and/or "subsurface" O. In the later stages the growing [1$\bar{1}$0] −Rh−O− chains cause segmentation and destruction of the [001] -Rh-N- chains and convert the substrate surface structure to a (1×2). The factors controlling these structural transformations are (i) the requirement of a critical coverage (≥0.1 ML) to initiate the O-(1×n) reconstruction and (ii) the accommodation of a dense N + O layer minimizing the repulsive interactions between the coadsorbates.

Figure 3.2 schematically illustrates the mechanism of displacement of the (2×1)-N islands with increasing N + O coverage derived from the STM results. The O adsorption site in a c(2×4) structure is chosen assuming that the antiphase zigzag motif in the STM images reflects the O arrangement in 3-fold sites along the [1$\bar{1}$0] rows. The arrangement of N is suggested in the recent LEED analysis of the system.[38] The most strongly affected by these structural transformations is the nitrogen chemisorption bond. Small amounts of O activate the formation of [001] −M−N− chains where nitrogen is strongly bonded. Transformation to a O-(1×2) phase eliminates the stabilization effect of the −Rh−N− chains and introduces repulsive forces which destabilize the N adsorption state. This indicates that in the later stages the energetic that governs the surface restructuring favors oxygen accommodation. The nitrogen from the c(2×4) phase can be easily desorbed leaving a (2×2)p2mg oxygen layer.[32] An interesting result also is the reduced reactivity of O in the c(2×4) structure with respect to H_2 oxidation, which is ascribed to deactivation effect of N on the H_2 dissociative adsorption.[38]

As will be shown in the following section, these first achievements in identifying the interplay between composition and structure at a microscopic scale have contributed to the understanding of variations in the surface reactivity and in the profiles of the chemical waves observed in the course of the surface reactions.

4. Surface Reactions Involving Reconstructions

4.1. General Remarks

In this section several classes of oxidation reactions, which involve adsorbate-induced reconstructions, will be discussed. These studies are of particular importance for revealing the reaction steps

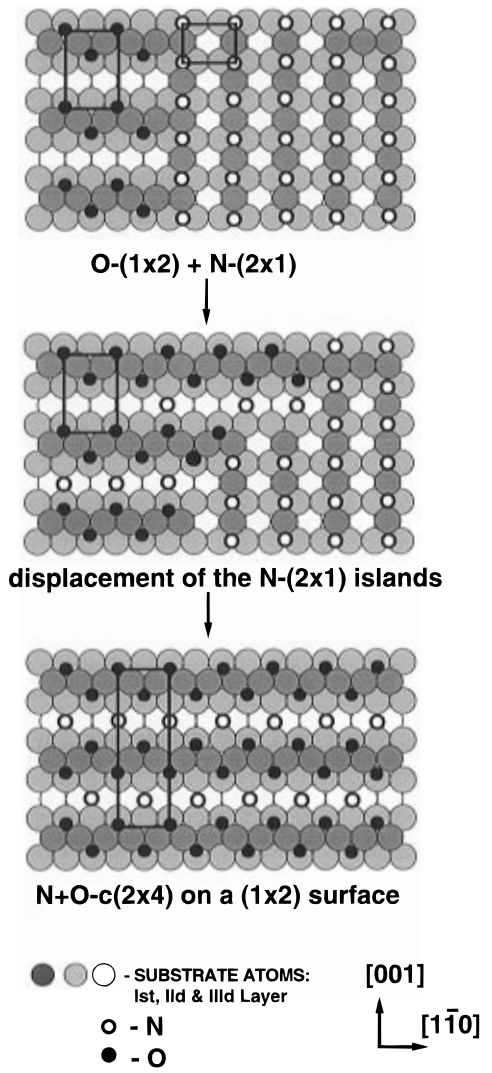

Figure 3.2. Model of the mass transport and tentative adatom arrangements involved in the structural transformation from a N-(2×1) + O-(1×2) to O + N-c(2×4) phase on Rh(110).

playing a crucial role in the structural-sensitive reactions. The emphasis will be on describing the impact of the reaction conditions (temperature and surface composition) on the local surface structure, which determines the kind and density of the active reaction centers and the local reaction rates. The simpler oxidation processes referred here are those where only O induces a surface restructuring under the reaction condition. The second class of oxidation reactions are those where, in addition to O, a second reaction species also favors a surface reconstruction.

All oxidation reactions reviewed here involve an O-(n×1) or an O-(1×n) reconstructed phase, where the density and the length of the −M−O− units vary with reaction conditions (temperature and reactants partial pressures). The role of the −M−O− units in the surface processes depends on the general reaction mechanism. When the oxidation reaction proceeds as a Langmuir−Hinshelwood (L−H) process, which is the most common case, the second species must adsorb on a O-free area and diffuse to a site adjacent to an active oxygen adatom. Thus a maximum reaction rate is expected at a lower oxygen coverage when shorter −M−O− chains prevail. When the oxidation reaction proceeds as a Eley−Rideal (E−R) process the reaction rate should increase with O coverage, i.e. a maximum reaction rate is expected at a high density of the −M−O− units. A consistent picture for the coverage sensitivity observed in L−H or E−R oxidation processes, where reconstructive chemisorption of oxygen is involved, has been derived on the basis of the STM reaction studies.[39−43]

4.2. Reactivity of the O-(n×1) and O-(1×n) Phases

The catalytic oxidation of CO, H_2, H_2S, and NH_3, considered in this section, represents several cases where only one of the reaction participants, namely O, restructures the surface under the reaction conditions. When these reactions are carried out on the fcc (110) surfaces of Cu, Ni, Ag, Rh, or Pd a common reaction step is the oxygen reconstructive chemisorption. The structural units of the induced (n×1) or (1×n) reconstructions are [001] −M−O− chains with O in long bridge sites or [1$\bar{1}$0] −M−O− chains with O in 3-fold sites along the rows, respectively (see Figures 2.1 and 2.2). The examples, discussed below, illustrate the following two typical cases: (i) reactions where the products immediately desorb; (ii) reactions where some of the products remain on the surface without disturbing the substrate structure.

4.2.1. CO and H_2 Reaction with O-(n×1) Phases

The oxidation reactions, described here, are L−H processes, where the reaction products, CO_2 and H_2O, immediately desorb under the actual reaction conditions. A common feature for all three substrates, Ni-(110), Cu(110), and Ag(110), is that the surface reactivity is influenced by the O-(n×1) reconstructive chemisorption and that the adsorption of the second reacting species, CO or H_2, requires an O-free surface space. At low O coverages the second species can adsorb on the clean areas between the spaced islands of −M−O− units and diffuse to the sites where O is located in order to react. When the −M−O− chain density is high the L−H oxidation reactions are inhibited, because of the absence of "free" substrate areas for adsorption of the second species. The inhibition is more dramatic in the case of dissociative chemisorption, e.g. H_2. This lack of a free adsorption space results in the often observed "induction" period which precedes the reactions.

The STM studies of CO and H_2 oxidation at low- and high-oxygen coverages have shed light on the microscopic reaction mechanism. The derived from the STM studies reaction mechanism for oxidation involving a O-(n×1) reconstructed phase is illustrated by the schematic models in Figure 4.1. Figure 4.1a shows the interactions after CO (H) adsorption at a low oxygen coverage when O-(2×1) and O-free (1×1) islands coexist. It has been evidenced that the most active reaction centers are the lower coordinated O atoms at the end of the −M−O− chains.[39−41] These active end points result from kinks of the island structure or from row termination. Their density is larger at lower O coverages when the −M−O− chains are shorter. The STM images have also evidenced that in some cases the second species, adsorbed on adjacent clean sites, might attack the −M−O− rows creating more active O-terminated ends.[35,39−41] Another interesting feature in the local mechanism of

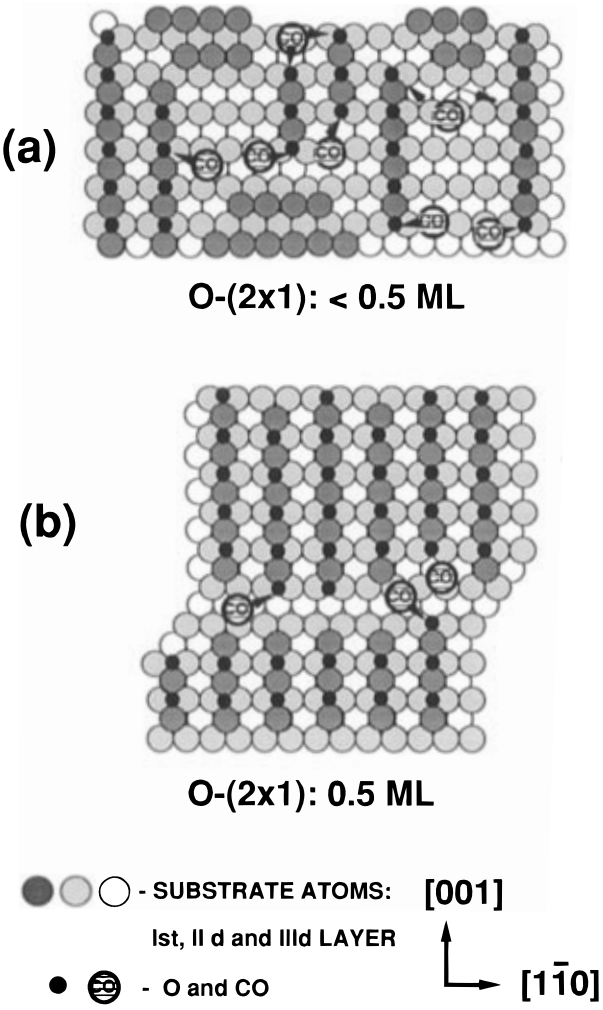

Figure 4.1. Schematic model of the L−H CO reaction with the −O−M− units of a O-($n\times1$) reconstructed phase. Panel a shows low-oxygen coverage where the CO adsorbed on an O-free islands attacks the −O−M− chains, preferentially at the O end points. The reactions propagates along the [001] rows. The released metal atoms migrate to the step edges enlarging the terraces of a (1×1) bare surface. Panel b shows high-oxygen coverage where an "induction" period is observed because only the step edges favor the CO adsorption.

these oxidation reactions is that, after initiation, the reaction continues in a highly anisotropic fashion progressing along the [001] −M−O− rows. The reconstruction is lifted when the oxygen, which stabilizes the [001] −M−O− chains, is reacted away. Since the reaction products, CO_2 and H_2O, immediately desorb this allows the released metal atoms to migrate undisturbed and aggregate at terrace edges resulting in growth of a restored flat (1×1) surface.

Figure 4.1b illustrates the initiation of a L−H oxidation process at a high oxygen coverage when the whole surface is covered by a O-(2×1) phase. Close inspection of the variations in the surface morphology during the "induction" period has shown that, when the terraces are saturated with −M−O− chains, the only "free" adsorption sites left are the step edges.[35,39] Thus, initially the adsorption of the second species can take place only at the step edges. An important observation is the anisotropic rate enhancement along the steps running in the [1$\bar{1}$0] and [001] directions. The reaction is predominantly initiated at steps edges oriented perpendicular to the −M−O− rows, where the active O-terminated ends are exposed: these are the steps running in the [1$\bar{1}$0] direction in the case of the ($n\times1$) reconstruction. Hence, the duration of the "induction" period is determined by the step density and orientation. Upon titration of oxygen at the step edges bare metal sites are created on the upper and lower terraces and the reaction rate is enhanced. Once larger O-free regions are formed (by reducing oxygen) the reaction continues according to the mechanism described above.

4.2.2. CO and H_2 Reaction with O-(1×n) Phases

The great variety of O reconstructed phases on Rh-(110) and the existence of an O unreconstructed phase at temperatures at which oxidation of CO and H_2 can occur offers an opportunity for systematic studies of the structural impact on the reactivity. As illustrated in the schematic models in Figure 2.2, the difference between the O-($1\times n$) reconstructed phases is in the number of [1$\bar{1}$0] rows between the missing [1$\bar{1}$0] rows, i.e. with increasing oxygen coverage the number of missing rows decreases. This reduces the surface concentration of oxygen adsorbed in the fcc 3-fold sites along the (1×2) troughs from 0.5 ML for the (2×2)p2mg structure on a (1x2) surface to 0.2 ML for the c(2×10) structure on a (1×5) surface. As outlined in section 2.4, oxygen is more deeply embedded in the fcc 3-fold sites along the (1×2) troughs because of the structural rearrangements in the Rh outermost layers. Conversion from the (2×2)p2mg to c(2×2n) structures leads to increasing population of the fcc 3-fold sites along the (1×1) troughs, where the bonding configuration of oxygen is similar to that of the unreconstructed O-(2×1)p2mg phase. As will be described below, the different bonding configuration of O along the (1×1) and (1×2) troughs exerts substantial influence on the reaction rates.

The first mass spectrometry reaction studies of the influence of oxygen structure on the reaction kinetics of CO and H_2 oxidation have revealed that the least reactive is the oxygen adsorbed along the (1×2) troughs.[44,45] Figure 4.2 presents the rate of CO_2 production at 298 K as a function of reaction time for different O structures with the same initial oxygen coverage: the O-(2×1)p2mg layer on an unreconstructed (1×1) surface reacts vigorously, whereas the O-(2×1)p2mg layer on an (1×2) reconstructed surface is practically unreactive at this temperature. The O-c(2×8) layer on a (1×4) reconstructed surface, which contains O adsorbed along the (1×1) and (1×2) troughs shows an intermediate reactivity with partial removal of oxygen at 298 K. The reconstructed phases become more reactive at higher temperatures which means that a higher activation barrier for reacting of oxygen along the (1×2) troughs exists.

These earlier studies of oxygen titration by CO or hydrogen have also shown that the oxygen-induced ($1\times n$) reconstructions can be preserved when the reaction is carried out at temperatures below 450 K.[46] Above 450 K the ($1\times n$) surface reverts to a (1×1) surface. This means that on Rh(110) the surface

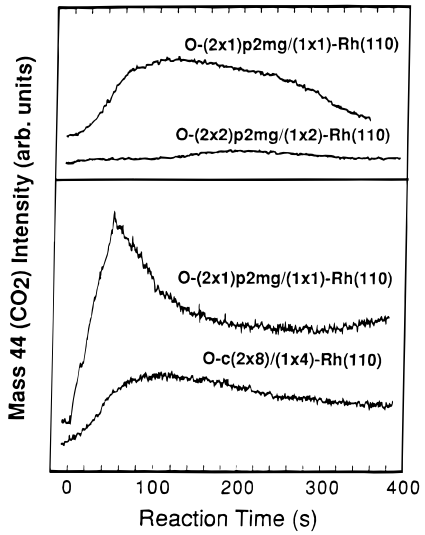

Figure 4.2. Rate of the CO_2 production at 298 K as a function of the reaction time for different O phases on an unreconstructed and reconstructed Rh(110) surfaces: top, initial O coverage of 0.5 ML, i.e. the O-(2×1)p2mg phase covers approximately half of the unreconstructed surface; bottom, initial O coverage of ~0.9 ML (ref 45).

structure of the O-freed areas varies with the reaction temperature. The temperature dependence of the surface structure left after oxygen titration distinguishes the oxidation reactions on Rh(110) from those on Cu, Ni, and Ag, where reacting off oxygen always lifts the (n×1) reconstruction. It is a general rule that the surface reactivity varies with different substrate surface structures. Recent studies have revealed that compared to adsorption on a (1×1)-Rh-(110) surface, the CO adlayers on a (1×2)-Rh(110) surface are less stable, whereas the H adlayers are more stable.[47,48] Undoubtedly, this structural dependence of the adsorptive properties has its impact on the reaction pathway and accounts for the observed structural sensitivity of CO oxidation at higher temperatures.[46]

The microscopic mechanism of CO oxidation on reconstructed (1×n)-Rh(110) surfaces, studied by STM, confirms the observed increase of the reactivity with decreasing the density of the (1×2) troughs: at room temperature the reacted O-c(2×8) areas are ~4 times more than the reacted O-c(2×6) areas and no reaction has been evidenced on the O-(2×2)p2mg regions.[43] Figure 4.3 illustrates schematically the reactivity of the different O-(1×n) phases at room temperature when the substrate reconstruction is preserved after oxygen removal. It is obvious that for all O-(1×n) phases formed on Rh(110) at O coverages ≥ 0.5 ML the step edges are the sole sites for initial CO adsorption. The higher reactivity of oxygen along the (1×1) troughs is the reason that the CO at step edges of the c(2×8) and c(2×10) areas reacts fastest.[38] Common features with the already described oxidation systems involving (n×1)-O reconstructions are: (i) the key role of step edges oriented perpendicular to the direction of the added/missing rows as adsorption and nucleation centers and (ii) the highly directional progressing of the reaction along the [1$\bar{1}$0] rows without affecting the neighboring structures across the (1×2) troughs.

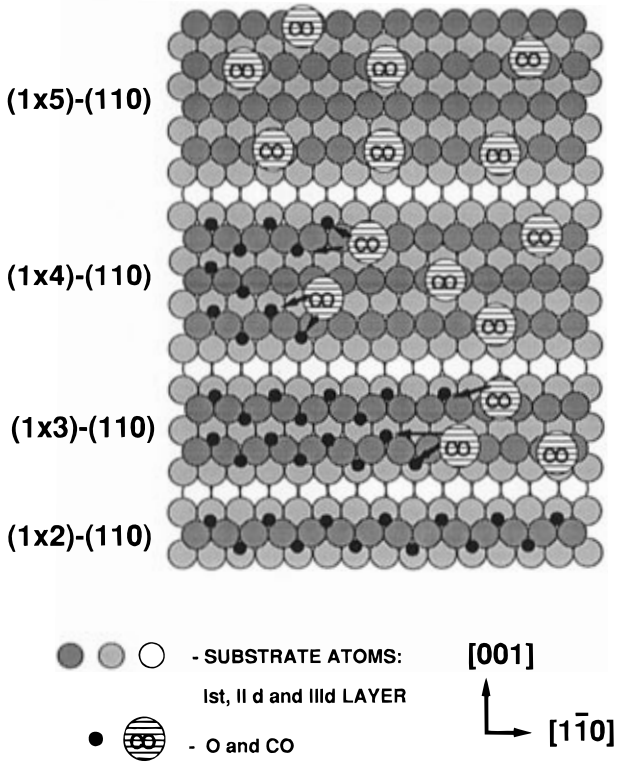

Figure 4.3. Schematic model of the L−H CO reaction with different O-(n×1) reconstructed phases on Rh(110), derived from STM data. It illustrates the enhancement of the directional reactivity going from a O-(1×2) to a O-(1×5) phase.

4.2.3. Oxidation of NH_3 and H_2S

The oxidation reactions, considered in subsections 4.2.1 and 4.2.2, result in products which immediately desorb under the actual reaction conditions. However, in many cases there are intermediates or products remaining on the surface which affect the reaction rate and the reaction mechanism without disturbing the substrate structure.

Typical examples for reactions where some of the products also adsorb but do not cause a reconstruction are NH_3 oxidation on Ni(110)[40] and H_2S oxidation on Cu(110).[43] The mechanism of these oxidation reactions has the following common features with the CO and H_2 oxidation processes, described above: (i) the O-terminated ends of the −M−O− chains are the most active centers; (ii) the reaction occurs in highly directional fashion along the −M−O− chains and (iii) the step edges serve as adsorption centers at a high −M−O− chain density. As illustrated in Figure 4.4, the difference is that some of the products do not desorb but accumulate on the surface in the course of the reaction: they are OH and NH_2 during NH_3 oxidation on the Ni(110) surface and S during H_2S oxidation on the Cu(110) surface. The increasing concentration of the products deactivates the surface, because they block the adsorption sites at the O-terminated ends and hinder the segmentation of the remaining Ni−O rows. The crowding on the surface also reduces the mobility of the substrate atoms released from the −M−O− chains: they cannot migrate to the terrace edges but agglomerate in islands increasing the roughness of the surface. Compared to CO and H_2, the NH_3 oxidation rate

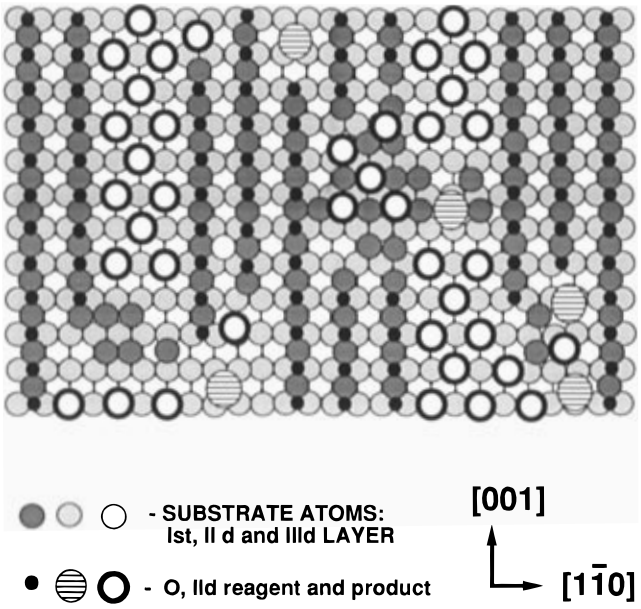

Figure 4.4. Schematic model of the mechanism of L−H reactions on a O-($n\times1$) reconstructed surface with adsorbed products. The latter block the sites at the active centers and impede the mobility of the IId reagent and the released substrate atoms.

shows a stronger oxygen coverage sensitivity and becomes zero at high oxygen coverages. This is related to the difference in the elementary reaction steps involved. Since NH_3 does not dissociate at a reaction temperature of 300 K, the only reaction pathway is a hydrogen-transfer reaction between NH_3 and O-edge atom of the Ni−O rows. This requires more O-terminated rows and a particular NH_3 adsorption configuration, which is difficult to be attained at the step edges.

4.3. Reactions Involving Two Reconstructed Phases

Typical examples for this class of reactions are H_2S oxidation on Ni(110),[33] NO reduction on Rh(110),[50−52] and NH_3 oxidation on Rh(110).[53] In all these cases, besides O, there is a second adsorbed species which also induces a reconstruction, e.g. S on Ni(110) and N on Rh(110). Provided the second species accumulate on the surface under the reaction conditions, the reaction pathway can be changed as well. In real systems such species can be deposited by contaminants, e.g. S in a steam re-forming reaction on Ni-based catalysts, which acts as a poison.

4.3.1. H_2S Oxidation on Ni(110)

Exposure of an O-(2×1) phase on Ni(110) to H_2S results in formation of H_2O which immediately desorbs, leaving S on the surface.[26] The STM experiments have shown that the mechanism of this reaction differs substantially from the mechanism of the L−H oxidation reactions described above. The main difference is that the O-terminated −Ni−O− rows do not act as active sites and the reaction proceeds in a homogeneous manner, i.e. there is no preferential initiation at the O end point of the −Ni−O− rows and step edges. The reason for this difference is that the H_2S oxidation on Ni(110) proceeds predominantly as an E−R process: interaction of impinging H_2S molecules with chemisorbed O independently on the O location within the −Ni−O− units. In principle the distribution of the species on the surface is very similar to that schematically presented in Figure 4.4. The only difference is the absence of a chemisorbed second reagent and of directional removal of O. After reduction of O the released Ni atoms form small (1×1) Ni islands, leaving randomly distributed (1×1) troughs behind which leads to surface roughening. S chemisorbs on these Ni-(1×1) regions forming S-c(2×2) islands. When the S deposit increases, the S-c(2×2) islands transform into an ordered S-(4×1) reconstructed phase. The preserved E−R reaction mechanism even when an O-free space is opened can be ascribed to the effect of the deposited S. H_2S decomposition on the bare Ni islands cannot supply H to react with the O-Ni chains, because S deactivates the surface for H adsorption.[14] Since the H_2S decomposition is a low activation energy process,[54] S adsorption on bare (1×1) Ni islands becomes a dominating reaction at low-oxygen coverages. An interesting observation is that the H_2S + O reaction leads to formation of a S-(4×1) reconstructed phase at room temperature, which is not possible during H_2S decomposition on an O-free Ni(110) surface. The difference in the surface morphology of the S-c(2×2) phase formed during the H_2S + O reaction (small island and troughs) and during the H_2S decomposition (large flat S-c(2×2) areas) suggests a higher surface energy for the rougher S-c(2×2) surface and a lower energy cost for its conversion into a S-(4×1) reconstructed phase.

4.3.2. NO Reduction by CO and H_2 on Rh(110)

NO reduction on a Rh(110) surface is an example of a reaction involving dissociation of a heteronuclear molecule to adatoms which favor reconstructions. As described in subsection 3.3 there is a competition between N and O to reconstruct the Rh(110) surface: N-($n\times1$) phases are initially formed whereas at high coverages an oxygen-induced (1×2) reconstruction becomes dominant resulting in destabilization of the nitrogen adsorption state. These structural transformations lead to substantial variations in the N_2 and CO_2 production rates in the initial stage of the CO+NO reaction on the Rh(110).[49] Figure 4.5 illustrates the out-of-phase changes in the rates of CO_2 and N_2 production, which are very pronounced when the reaction is carried out at 450−550 K. The rate variations of N_2 production correlate with the stability of the N adlayers, which is the highest for the (3×1) and (2×1)-N reconstructed phases. The rate of CO_2 production changes in opposite direction and also correlates with the observed structural changes. There is an initial induction period in the CO_2 production, which becomes longer at higher temperatures. The likely reason for the induction period is the lack of active adsorbed oxygen, because of the subsurface penetration of the first oxygen doses introduced by NO dissociation on a fresh catalyst. Obviously this process is favored at higher temperatures. After the induction period the rate variations of CO_2 production can be associated with the different reactivity of oxygen on unreconstructed and reconstructed surfaces. The lowest reactivity of the pure

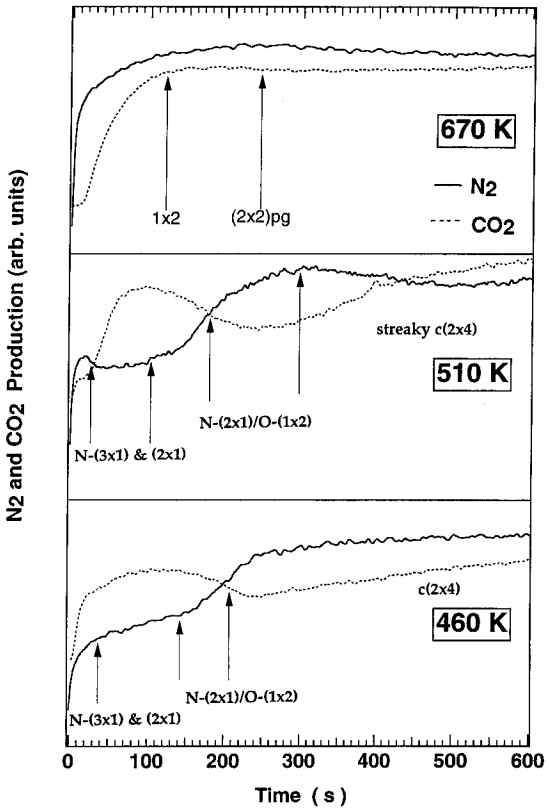

Figure 4.5. Changes in the rates of the N_2 (solid line) and CO_2 (dashed line) production on Rh(110) as a function of CO + NO reaction time for different reaction temperatures. The arrows indicate the changes in the surface structure in the course of the reaction (ref 50).

O-(1×2) phase accounts for the minimum observed when the surface is covered by separated (2×1)-N and (1×2)-O islands. At 670 K, with an exception of the initial induction period in the rate of CO_2 production, the kinetic curves of both products follow the same trend. This is due to the fact that at this temperature the surface retains no nitrogen and the surface structure and reactivity are determined only by the amount of adsorbed oxygen. In the particular reaction conditions the reaction rate grows until steady state characterized by an O-(2×2)p2mg surface.

The coverage dependence of the structural transformations in mixed O+N layers also accounts for the varying anisotropy along the chemical wave profile observed in the catalytic NO + H_2 reaction on Rh-(110).[51,52] This phenomenon, illustrated in Figure 4.6, is ascribed to the structural effects on the surface diffusion of the mobile adsorbates. A transition from elliptical to square-shaped chemical waves has been observed by changing the temperature and the NO/H_2 partial pressure. This is related to the structural variations induced by changing the reaction conditions. The elliptical pattern is the most usual reaction front shape (Figure 4.6(a)). It is elongated in the [1$\bar{1}$0] direction, as expected from the simple diffusion anisotropy along the two crystallographic directions: faster along the "smoother" [1$\bar{1}$0] direction. When the surface contains N-(2×1) and O-(1×2) reconstructed phases the anisotropy changes as the reaction front propagates and results in nucleation and growth of unusual square-shaped waves (Figure 4.6, parts a and b). Such dependence of the diffusion anisotropy on the local surface structure should be quite common and should account for the various oscillation patterns observed in the chemical reactions.

4.3.3. NH_3 Oxidation on Rh(110): Formation of an Intermediate Reconstructed Phase

In the last system considered in this survey, the reaction of NH_3 with a O-c(2×8) phase on Rh(110), a formation of a metastable surface phase has been evidenced. This phase mediates the conversion between two stable O- and N- reconstructed phases. It represents a "true" reaction intermediate which cannot be formed by either of the reaction participants alone. Figure 4.7 illustrates these structural transformations evidenced by STM studies.

The initial O-c(2 × 8) layer is formed on a (1 × 4) reconstructed surface (Figure 4.7a). Reduction of O by reaction with NH_3 at 380 K leaves only adsorbed N and results in a new surface morphology: the structural units are short segments of [001] rows resembling the −Rh−N− chains observed on a N-(*n*×1) reconstructed surface (Figure 4.7, parts b and

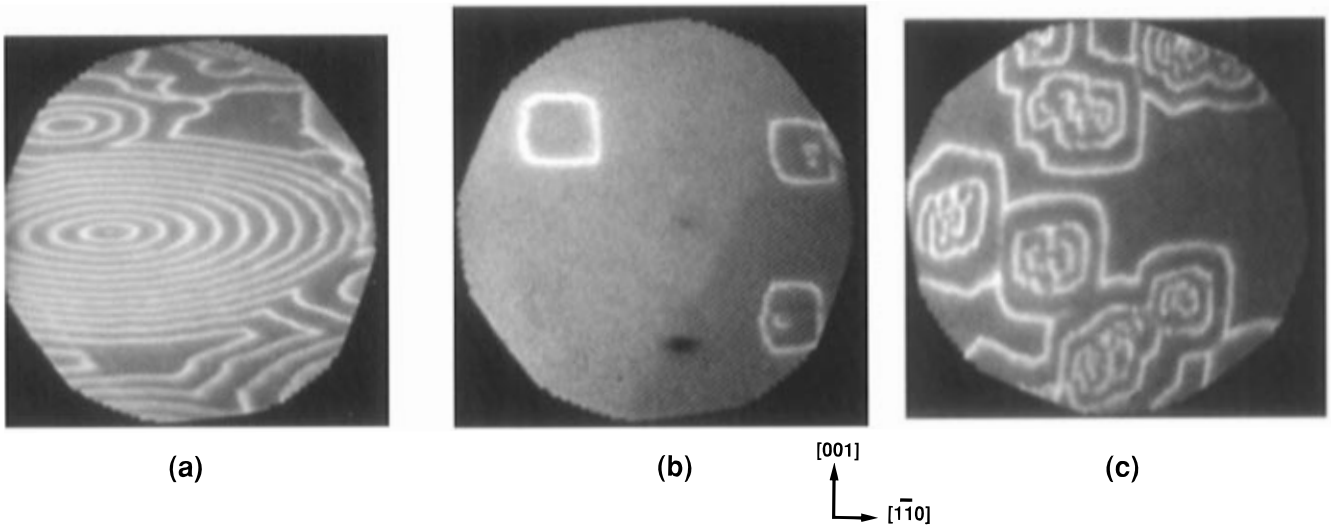

Figure 4.6. PEM micrographs showing the geometry of chemical waves observed during the NO + H_2 reaction on Rh-(110) carried out under reaction conditions which favor different surface structures.[47] The variation in the shape of the chemical waves reflects the influence of the N and O reconstructive chemisorption (ref 51).

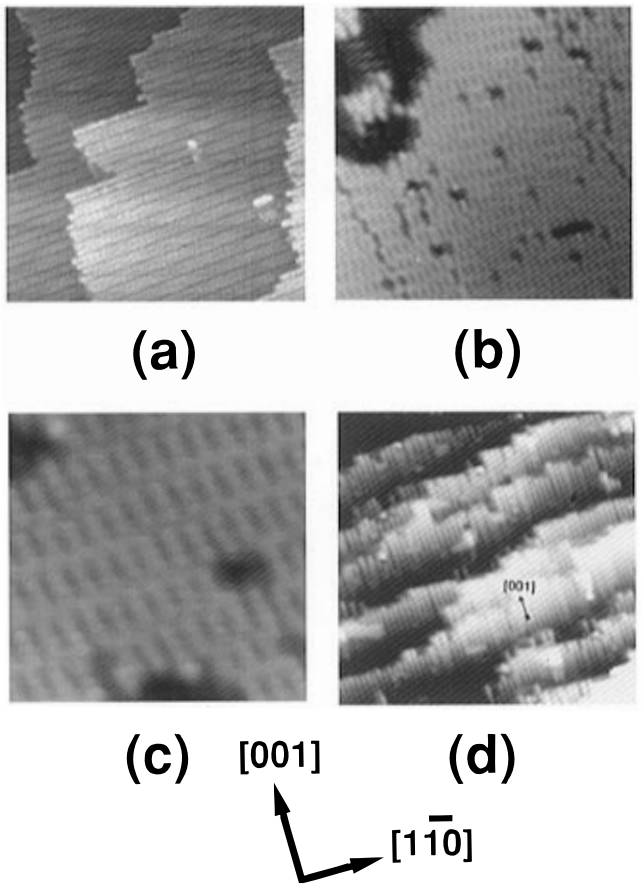

Figure 4.7. (a) STM image of the initial O-c(2 × 8) structure on Rh(110). (b and c) Low- and high-resolution STM images of the trimer intermediate structure obtained after O reduction at 380 K. (d) STM image of the N-(2×1) surface obtained after heating the "trimer" surface to 450 K.

c). The segments contain three Rh atoms and are named trimers. The trimers of the adjacent arrays, arranged in a zigzag fashion along the [001] direction, result in a hexagonal superlattice with an overall symmetry of c(2×6). The trimer-c(2×6) structure can be converted to a N-(2×1) structure by annealing to 450 K (Figure 4.7d). This indicates that the trimer structure mediates the conversion from the (1×4) to a (2×1) reconstructed phase.

These STM results suggest that after removal of O the anisotropy of the metastable (1×4) substrate structure constrains the N-reconstructive interactions within the top layer Rh [1$\bar{1}$0] rows. Models to illustrate this effect are shown in Figure 4.8. On energetic grounds associated with reduction of the repulsive N−N interactions on the (1×4) surface, the bridge-bonded N should be placed on alternating [001] Rh rows along the (1×2) troughs (Figure 4.8a). This morphology influences the further structural transformations and explains the presence of the zigzag-arranged trimer features. N tends to optimize its bonding by initiation of a local (2×1) reconstruction of the top (1×4) Rh layer. The morphology and the composition (N coverage of 0.5 ML) of the intermediate trimer structure, illustrated in Figure 4.8b, indicates that the local (2×1) restructuring of the (1×4) surface should be accompanied by sliding of the [001] Rh−N rows in the [001] direction to fill the missing [1$\bar{1}$0] rows. This intermediate trimer

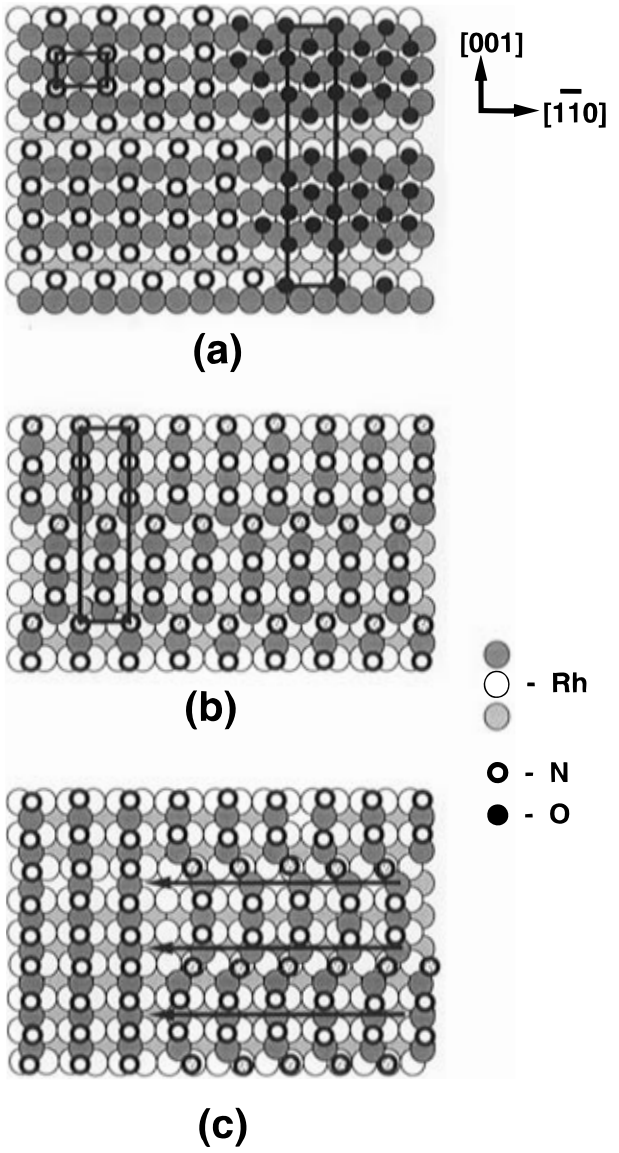

Figure 4.8. Model of the microscopic mechanism of the O-(1×4) to N-(2×1) conversion mediated by the metastable trimer structure: (a) the first stage of titration of the O-c(2×8) phase and deposition of N; (b) the trimer-c(2×6) structure; (c) the trimer-c(2×6) to N-(2×1) phase transition, where the mass transport is facilitated by heating to 450 K.

structure is relatively stable, which we attribute to the stability and the low mobility of the Rh−N trimers. The morphology of this structure indicates that at a nanoscale, the mass transport is strongly influenced by the initial structural anisotropy of the surface and by the constrained mobility in one of the crystallographic directions. Conversion to the final (2×1) structure (Figure 4.8c) requires an activation energy to shift the trimers one lattice distance in the [1$\bar{1}$0] direction, which is gained by heating to 450 K.

This recent study on the structural transformations of a Rh(110) surface during ammonia oxidation illustrates how complicated the processes can become when the reaction participants favour substrate structural changes. Metastable surface structures can be formed in the course of the surface reactions which mediate the structural transformations induced by the reaction participants. These intermediate structural phases with poorly defined properties

might cover a substantial fraction of the surface and exert specific effects on the surface reactivity.

4.4. Conclusions

The reviewed results for the microscopic mechanism of several oxidation reactions clearly illustrate a reactivity strongly influenced by the oxygen-induced reconstructions on the surface, which generally occurs during oxygen chemisorption on transition metal surfaces. The selected oxidation reactions involving O-induced ($n\times1$) or ($1\times n$) reconstructions of fcc (110) metal surfaces exhibit several common features of the local reaction mechanism. The most important findings can be summarized as follows.

For oxidation reactions which proceed as a L−H process the type of the "active" reaction sites and the nature of the intermediate steps have been revealed. First, the reactions always proceed in a heterogeneous manner because the active reaction sites are the O end points of the −M−O− chains. This means that the density of the O-terminated −M−O− units of the reconstructed phase is a controlling factor for the reaction rate. This finding explains why the oxidation reaction rates are not simply proportional to the O surface concentration: they pass through a maximum at rather low O coverages of ∼0.2 ML, when shorter −M−O− chains dominate. The second finding is the anisotropic propagation of the reaction front, i.e. the reaction rate is much faster along the crystallographic direction of the −M−O− chains, i.e. [001] in the case of O-($n\times1$) reconstructions and [1$\bar{1}$0] in the case of O-($1\times n$) reconstructions. This directional reactivity can be associated with the O concentration anisotropy along these crystallographic directions. The third finding concerns the phenomenon "induction" period at high oxygen coverages, when the surface is saturated by −M−O− chains. In this case the sole adsorption sites for the second reagent are the step edges. The reactions on an O-saturated surface also proceed heterogeneously with preferential initiation at the step edges oriented perpendicularly to the −M−O− rows, where the active O end points are exposed. The duration of the "induction" period and the initial reaction rate depend on the density of steps with a favorable orientation. The forth finding concerns the cases of adsorbed intermediates or products which commonly results in deactivation. When the adsorption of these species is not of a reconstructive type they affect the reaction rate simply by blocking the sites at the O-active centers and constraining the mobility of the adspecies on the surface and released metal atoms. When the intermediates or products also form a reconstructed phase the local surface structure varies with the adsorbate coverage and temperature. The surface structure of the areas after oxygen reduction can also vary: mass transport of the released substrate atoms to restore the (1×1) phase or preservation of the reconstructed phase are possible depending on the reaction temperature. These local transformations of the structure during surface reactions generate rather complicated variations in the reactivity and selectivity. Large changes in the mobility of the species, in the local reaction rates and in the propagation of the reaction front are quite common and account for the structural sensitivity observed in many catalytic reactions.

The second class, namely E−R oxidation processes, are rare and microscopic studies of the intermediate steps at the surface are very scarce. The main differences in the microscopic mechanism of this class of oxidation reactions, evidenced by the STM studies, is that (i) they proceed in a homogeneous manner; (ii) they do not exhibit an one-dimensional reactivity, and (iii) their reaction rate is a simple function of the −M−O− chain density. These differences arise because the reaction rate is controlled by the collisions of gas molecules with the chemisorbed oxygen, independent of its location. Hence, the O end points of the −M−O− chains have no importance as active centers and there is no need of an O-free space for the second reagent.

5. Summary and Outlook

The most recent powerful new developments in surface science have provided us with a reliable approach to surface structure and chemical reactivity at a nanometer and atomic level. It has already been shown in atomic detail the rearrangements of the surface atoms that accompany surface processes. In the recent few years the achievements in revealing the mechanism and the controlling factors of a surface reconstruction induced by adsorbates have provided the basis for understanding the influence of the surface structure on the chemical reactivity. Insight into the microkinetics of several oxidation catalytic reactions occurring on single-crystal metal surfaces have revealed at an atomic level: (i) the kind and the location of the active sites, (ii) the role of the surface structural defects and mass transport (e.g., step edges, kinks, etc), and (iii) the local variations in surface structure and composition during surface reactions, etc. A fairly novel finding is the impact of the surface structure on the reaction front propagation resulting in a directional anisotropy of the reaction rates.

Looking into the close future nanoscale reaction studies of many other important industrial processes have to be carried out. Also for the simple oxidation reactions reviewed here more comprehensive information about the factors that influence bond breaking and bond formation on the surface is needed. After this information is gained, more general conclusions about the type of the active sites and about the controlling factors in the relation structure−reactivity can be drawn.

Although studies of surface reactions on well-defined surfaces are considered as far from "real" catalysis, the information that they provide are building the basis for future design of catalysts with desired properties. The knowledge gained at a microscopic scale with model systems will define the active site structure, the relation of local surface composition and structure−bond strengths, and mobility of the reacting species. All these factors are controlling the surface reactions and are directly related to the catalyst reactivity and selectivity.

6. Acknowledgments

I would like to acknowledge F. Bessenbacher and R. Imbihl for their kindness to provide their recent results and illustrations included in the present review. It is a pleasure to thank my collaborators and colleagues who contributed to this work: A. Baraldi, M. Bowker, G. Comelli, V. R. Dhanak, F. M. Leibsle, S. Lizzit, P. W. Murray, G. Paolucci, K. Prince, R. Rosei, and G. Thornton.

7. References

(1) (1) Flytzani-Stephanopopoulos, M.; Schmidt, L. D. *Prog. Surf. Sci.* **1979**, *9*, 83.
(2) Ertl, G. *Langmuir* **1987**, *3*, 4; *Science* **1991**, *254*, 1750
(3) Imbihl, R.; Ertl, G. *Chem. Rev.* **1995**, *95*, 697.
(4) Phase Transitions and Adsorbate restructuring at Metal Surfaces. *The Chemical Physics of Solid Surfaces*; King, D. A., Woodruff, D. P., Eds.; Elsevier: Amsterdam, 1994; Vol. 7.
(5) Somorjai, G. A.; Van Hove, M. A. *Prog. Surf. Sci.* **1989**, *30*, 201.
(6) Wintterlin, J.; Behm, R. J. In *Scanning Tunneling Microscopy*; Guntherodt, H. J., Wiesendanger, R., Eds.; Springer Series in Surface Science 20; Springer Verlag: Berlin, 1992; Chapter 4.
(7) Bernasconi, M.; Tosatti, E. *Surf. Sci. Rep.* **1993**, *17* (7/8), 99.
(8) Estrup, P. J. In *Chemistry and Physics of Solid Surfaces V*; Vanselowe, R., Howe, R., Eds.; Springer-Verlag: Berlin, 1984; p 205.
(9) Thiel, P. A.; Estrup, P. J. In *The Handbook of Surface Imaging and Visualization*; Hibbard, A. T., Ed.; CRC Press: Boca Raton, FL, 1995; Chapter 29, p 407.
(10) *Scanning Tunneling Microscopy*; Guntherodt, H. J., Wiesendanger, R., Eds.; Springer Series in Surface Science 20; Springer Verlag: Berlin, 1992.
(11) Engel, W.; Kordesch, M. E.; Rotermund, H. H.; Kubala, S.; Oertzen, A. v. *Ultramicroscopy* **1991**, *36*, 148.
(12) Taylor , H. S. *Proc. Royal Soc. London* **1925**, *A 108*, 105.
(13) Bonzel, H. P.; Duckers, K. *Chemistry and Physics of Solid Surfaces*. Springer Series in Surface Science 10; Springer-Verlag: Berlin, 1988; p 429.
(14) Kiskinova, M. *Poisoning and Promotion in Catalysis Based on Surface Science Concepts and Experiments*; Delmon, B., Yates, J. T., Eds.; Elsevier: Amsterdam, 1992; Vol. 70.
(15) Besenbacher, F.; Norskov, J. K. *Prog. Surf. Sci.* **1993**, *44*, 5.
(16) Coulman, D. J.; Wintterlin, J.; Behm, R. J.; Ertl, G. *Phys. Rev. Lett.* **1990**, *64*, 1761.
(17) Feidenhans, R.; Grey, F.; Nilsen, M.; Besenbacher, F.; Jensen, F.; Laegsgaard, E.; Stensgaard, I.; Jacobsen, K. W.; Norskov, J. K.; Jonson, R. L. *Phys. Rev. Lett.* **1990**, *65*, 2027.
(18) Kern, K.; Niehus, H.; Schatz, A.; Zeppenfeld, P.; Goerge, J.; Comsa, G. *Phys. Rev. Lett.* **1991**, *67*, 855.
(19) Eirdal, L.; Besenbacher, F.; Laegsgaard, E.; Stensgaard, I. *Ultramicroscopy* **1992**, *42*−*44*, 505.
(20) Hashizume, T.; Taniguchi, M.; Motai, K.; Lu, H.; Tanaka, K.; Sakurai, T. *Surf. Sci.* **1992**, *266*, 282.
(21) Murray, P. W.; Leibsle, F. M.; Li, Y.; Guo, Q.; Bowker, M.; Thornton, G.; Dhanak, V. R.; Prince, K. C.; Rosei, R. *Phys. Rev. B* **1993**, *47* 12976.
(22) Tanaka, H.; Yoshinobu, J.; Kawai, M. *Surf. Sci.* **1995**, *327*, L505.
(23) Niehus, H.; Spitz, R.; Besocke, K.; Comsa, G. *Phys. Rev. B* **1991**,*43*, 12619.
(24) Leibsle, F. M.; Davis, R.; Robinson, A. V. *Phys. Rev. B* **1993**, *47*, 100052.
(25) Voetz, M.; Niehus, H.; O'Connor, J.; Comsa, G. *Surf. Sci.* **1993**, *292*, 211.
(26) Murray, P.; Leibsle, F. M.; Thornton, G.; Bowker, M.; Dhanak, V. R.; Baraldi, A.; Kiskinova, M.; Rosei, R. *Surf. Sci.* **1994**, *304*, 48.
(27) Ruan, L.; Stensgaard, I.; Lænsgaard, E.; Besenbacher, F. *Surf. Sci.* **1993**, *296*, 275.
(28) CRC Handbook of Chemistry and Physics, 71th ed.; CRC Press Inc., Boca Raton, FL, 1992; p 9−123.
(29) Jacobsen, K. W.; Norskov, J. K. *Phys. Rev. Lett.* **1990**, *65*, 1788.
(30) Gierer, M.; Over, H.; Ertl, G.; Wohlgemuth, H.; Schwarz, E.; Christmann, K. *Surf. Sci. Lett.* **1993**, *297*, L73.
(31) Alfe, D.; Rudolf, P.; Kiskinova, M.; Rosei, R. *Chem. Phys. Lett.* **1993**, *211*, 220. Comelli, G.; et al. *Chem. Phys. Lett.*, submitted for publication.
(32) Kiskinova, M.; Comelli, G.; Lizzit,S.; Paolucci, G.; Rosei, R. *Appl. Surf. Sci.* **1993**, *64*, 185.
(33) Ruan, L.; F. Besenbacher, F.; Stensgaard, I.; Laegsgaard, E. *Phys. Rev. Lett.* **1992**, *69*, 3523.
(34) Leibsle, F. M.; Davis, R.; Robinson, A. W. *Phys. Rev. B* **1993**, *47*, 100052.
(35) Sprunger, P. T.; Okawa, Y.; Besenbacher, F.; Stensgaard, I.; Tanaka, K. *Surf. Sci.* in press.
(36) Murray, P. W.; Thornton, G.; Bowker, M.; Dhanak, V. R.; Baraldi, A.; Rosei, R.; Kiskinova, M. *Phys. Rev. Lett.* **1993**, *71*, 4369.
(37) Dhanak, V. R.; Baraldi, A.; Rosei, R.; Kiskinova, M.; Murray, P. W.; Thornton, G.; Bowker, M. *Phys. Rev. B* **1994**, *50*, 8807.
(38) Gierer, M.; Mertens, F.; Over, H.; Ertl, G.; Imbihl, R. *Surf. Sci. Lett.* **1995,** *339*, L903
(39) Murray, P. W.; Besenbacher, F.; Stensgaard, I. *Isr. J. Chem.* **1995**, in press.
(40) Ruan, L.; Stensgaard, I.; Laegsgaard, E.; Besenbacher, F. *Surf. Sci.* **1994**, *314*, L873.
(41) Crew, W. W.; Madix, R. J. *Surf. Sci.* **1994**, *319*, L34.
(42) Leibsle, F. M.; Murray, P. W.; Francis, S. M.; Thortnton, G.; Bowker, M. *Nature* **1993**, *363*, 706.
(43) Besenbacher, F.; Sprunger, P. T.; Ruan, L.; Olesen, L.; Stensgaard, I.; Lægsgaard, E. *Top. Catal.* **1994**, *1*, 325.
(44) Bowker, M.; Guo, Q.; Joyner, R. W. *Surf. Sci.* **1993**, *280*, 50.
(45) Comelli, G.; Dhanak, V. R.; Kiskinova, M.; Paolucci, G.; Prince, K. C.; Rosei, R. *Surf. Sci.* **1992**, *260*, 7; **1992**, *269*−*270*, 360.
(46) Dhanak, V. R.; Comelli, G.; Paolucci, G.; Kiskinova, M.; Prince, K. C.; Rosei, R. *Chem. Phys. Lett.* **1992**, *1888*, 237.
(47) Baraldi, A.; Dhanak, V. R.; Comelli, G.; Kiskinova, M.; Rosei, R. *Surf. Sci.* **1993**, *293*, 246.
(48) Dhanak, V. R.; Baraldi, A.; Comelli, G.; Paolucci, G.; Kiskinova, M.; Rosei, R. *Surf. Sci.* **1993**, *295*, 287.
(49) Bowker, M.; Guo, Q.; Joyner, R. W. *Catal. Lett.* **1993**, *18*, 119.
(50) Baraldi, A.; Dhanak, V. R.; Comeli, G.; Kiskinova, M.; Rosei, R. *Appl. Surf. Sci.* **1993**, *68*, 395.
(51) Mertens, F.; Imbihl, R. *Nature* **1994**, *370*, 124.
(52) Gottschalk, N.; Mertens, F.; Bar, M.; Eiswirth, M.; Imbihl, R. *Phys. Rev. Lett.* **1994**, *73*, 3483.
(53) Kiskinova, M.; Dhanak, V. R.; Baraldi, A.; Thornton, G.; Bowker, M.; Leibsle, F. M.; Rosei, R. *Phys. Rev. B* **1995**, *52*, 1532
(54) Huntley, D. R. *Surf. Sci.* **1990**, *240*, 13.

CR950226Y